Journal of Insect Physiology 55 (2009) 869–884

Contents lists available at ScienceDirect

Journal of Insect Physiology

journal homepage: www.elsevier.com/locate/jinsphys

The AC–DC Correlation Monitor: New EPG design with flexible input resistors to detect both R and emf components for any piercing–sucking hemipteran☆

Elaine A. Backus [a,*], William H. Bennett [b]

[a] USDA Agricultural Research Service, Crop Diseases, Pests and Genetics, San Joaquin Valley Agric. Sciences Ctr., 9611 So. Riverbend Ave., Parlier, CA 93648, USA
[b] Electronic Instrument Laboratory, University of Missouri (retired), 7441 Elkstown Rd., Otterville, MO 65348, USA

ARTICLE INFO

Article history:
Received 25 February 2009
Received in revised form 19 May 2009
Accepted 19 May 2009

Keywords:
Feeding
Electrical penetration graph
Electronic monitoring of insect feeding
Aphid
Acyrthosiphon pisum
Insecta

ABSTRACT

Much of what is known today about hemipteran feeding biology, as well as mechanisms of their host plant interactions and transmission of phytopathogens, has been learned via use of electrical penetration graph (EPG) technology, originally called electronic monitoring of insect feeding. Key to all of this information has been the electronic designs of EPG monitors. It has been 45 years since the publication of the original EPG, the AC monitor, and 30 years since introduction of the DC monitor, an important improvement for EPG science. Herein we describe our new AC–DC Correlation Monitor, the first major improvement in design since the DC monitor. We provide the monitor's block diagram and circuit description, and discuss (as a first example) its application to aphid feeding waveforms. Our instrument combines design features from the existing AC Missouri monitor and the DC Tjallingii monitor, plus several new innovations. It can produce three simultaneous, time-synchronized, output signals from a single insect, via AC and DC signal processing circuitry, as well as using either AC, DC, AC-plus-DC, or 0 V substrate voltage. Our research conclusively demonstrates that AC signal processing can be designed to duplicate the level of detail and fidelity of aphid waveforms previously provided solely by the DC monitor, including all R- and emf-component waveforms. Availability of either AC or DC applied voltages will allow similar high-resolution recording of insects that appear to be sensitive to DC applied voltages. We also begin to determine the subtle reasons why published waveforms from older AC and DC monitors appear to differ so greatly. Our instrument is a single, flexible, universal monitor that can provide maximum, R-plus-emf waveform information from any piercing–sucking species, especially non-aphid species with sensitivity to DC applied voltage.

Published by Elsevier Ltd.

1. Introduction

The study of hemipteran feeding was revolutionized in 1964 by McLean and Kinsey's publication of an "electronic measurement system" (McLean and Kinsey, 1964; McLean and Weigt, 1968) (later termed "electronic monitoring system" or EMS [Backus, 1994]) that made a feeding aphid part of an electrical circuit (McLean and Kinsey, 1964). Prior to that, it was not possible to identify in real-time the start of an aphid probe, let alone the highly specialized and detailed behaviors occurring otherwise invisibly during stylet penetration (probing) inside the plant. Since then, electronic monitoring of hemipteran feeding has revealed much of what is known today about these insects' feeding biology, as well as mechanisms of phytopathogen transmission and host plant interactions, especially for aphids. Key to all of this information has been the electronic designs of monitors.

McLean and Kinsey's (1964) early system used common technology of the day, i.e. amplitude modulation (AM) with an alternating current (AC) carrier wave applied to the plant, a relatively insensitive (10^6 Ohm [Ω] or one megohm) input resistor (Ri), and a slow-response strip chart recorder. This earliest system probably detected only the variable resistance to the applied carrier wave that was caused by various aphid feeding behaviors (reviewed in Walker, 2000; Backus et al., 2000). Fourteen years later, a major improvement was introduced. Tjallingii (1978) described a system using a direct current (DC) voltage applied to the plant (hereafter, AC or DC applied voltages are referred to as substrate voltages), and a more sensitive (10^9 Ω or one gigohm) input resistor. His system provided the added ability to detect biopotentials, which he termed the emf (electromotive force) component, generated in the insect–plant interface, in addition to

☆ *Disclaimer*: Mention of trade names or commercial products in this article is solely for the purpose of providing specific information and does not imply recommendation or endorsement by the U.S. Department of Agriculture.

* Corresponding author. Tel.: +1 559 596 2925.
E-mail addresses: elaine.backus@ars.usda.gov (E.A. Backus), ccbillb@hughes.net (W.H. Bennett).

0022-1910/$ – see front matter. Published by Elsevier Ltd.
doi:10.1016/j.jinsphys.2009.05.007

resistance changes, which he termed the R component (Tjallingii, 1985, 1988). Detection of biopotential information provided crucial information about aphid waveforms, most importantly the now well-studied intracellular punctures, represented by the potential drop (pd) waveform (Tjallingii, 1985, 1988; Walker, 2000). Tjallingii (1985) also renamed the instrument, calling it the "electrical penetration graph" (EPG). Since then, the two systems have come to be termed the AC and DC EPG systems, respectively. Herein, we will use the terms 'system' to indicate these broad categories, and 'monitor' to describe specific AC or DC system designs.

In the time since 1964, at least seven major AC monitor designs have been published (described in Backus et al., 2000), while the single, simpler DC system design has had only minor adjustments since 1978. A major improvement in AC design was the Missouri monitor (v. 1.0, Backus and Bennett, 1992). At the same time, researchers began to use computerized, analog-to-digital (A/D) display and recording of waveforms from both AC and DC systems. Both AC and DC users now have abandoned the use of strip chart recorders used by early AC system studies, justifiably criticized by Tjallingii (1995). The Missouri monitor, combined with computerized display, allowed more waveform detail to be displayed than in previous AC system publications (Reese et al., 2000).

During this 45-year evolution of instrument design, EPG monitors became somewhat specialized for different insects; DC system users primarily studied sternorrhynchans (mostly aphids, but a few whiteflies [Janssen et al., 1989; Walker and Janssen, 2000], mealybugs [Calatayud et al., 2001], and phylloxera [Kingston, 2007]), as well as thrips (Harrewijn et al., 1996; Kindt et al., 2003). The AC system has been used not only for most studies of auchenorrhychans (especially leafhoppers [Serrano et al., 2000; Wayadande and Nault, 1993], but also for some planthoppers [Velusamy and Heinrichs, 1986]) and heteropterans (Bonjour et al., 1991; Backus et al., 2007) (complete bibliography 1964–1990 in Backus, 1994). Recent studies of auchenorrhynchans have been performed with the DC system, e.g. leafhoppers (Kimmins and Bosque-Perez, 1996; Lett et al., 2001; Stafford and Walker, 2009; Stafford et al., 2009; Miranda et al., 2009) and planthoppers (Buduca et al., 1996). However, based on the design of the applied voltage circuit in the DC monitor, it is usually not known how much DC voltage is applied to the plant/insect preparation. When measured, it was often low or zero voltage (e.g. Lett et al., 2001). Recent observations by Backus (unpublished data) suggest that AC vs. DC substrate voltages may be differentially tolerated by these insects, for unknown reasons. When $10^9\ \Omega$ input resistors were used to increase sensitivity to emf, aphids were irritated by all but very low voltages (~10 mV) of applied AC. (Therefore, to perform the studies described herein, only 5 mV AC was used, with very high gain.) In contrast, *Homalodisca* sharpshooter leafhoppers (Cicadellidae: Cicadellinae) were irritated by similarly very low voltages of applied DC with $10^6\ \Omega$ input resistors (unpublished data). Both types of insects were unwilling to complete their probes when irritated. Future research will more rigorously test the hypothesis that sternorrynchans are sensitive to AC while auchenorrhynchans are sensitive to DC, at various amplifier sensitivities.

In symposium proceedings (Walker and Backus, 2000), both Tjallingii (2000) and Backus et al. (2000) end their review chapters by discussing the virtues of developing a "universal" monitor that could use both AC and DC signal processing circuitry, to provide the advantages of both systems and eliminate the disadvantages of each. A "universal amplifier" would "provide a useful combination for future research and development of EPG recording, and turn present controversy into collaboration" (Tjallingii, 2000). Tjallingii's proposed AC design was an "optimized AM device" which, in theory, would provide waveforms consisting of pure R components for each waveform type. This was an interesting attempt to derive benefit from a misunderstanding (i.e. that AC signal processing could not detect emf, and therefore its only useful application would be to emphasize R [Tjallingii, 2000]). However, when such a device was built (the first AC–DC monitor) and used for a study of thrips feeding (Kindt et al., 2006), it provided little new information and was not considered successful by the authors (see Section 4). Because this AM device was a simple attempt to merge two long-standing designs (the old AC and DC systems), we do not consider it a major advancement in EPG technology. Although our design is quite different from Tjallingii's AC–DC monitor, we ultimately share the same goal of developing a universal monitor. We hope that it can unify all EPG research with one, highly flexible and modern instrument.

There is now a strong need to apply modern EPG technology to a wider array of arthropod test subjects than in the past. To do so, a new, more flexible and electronically updated monitor design was necessary. The objective of this paper is to describe our AC–DC Correlation Monitor, the first true technical advancement in EPG designs in 30 years. The primary purpose of our design is to provide maximum flexibility in settings, so that users can empirically determine the optimal voltage type, input impedance, and signal processor type for the specific arthropod they are studying. The new monitor is a universal EPG instrument that provides identical, highly detailed waveforms using either AC or DC applied voltage, or both. It also offers switchable input resistors and other flexible design features, so that the user can empirically determine optimal settings for highly variably sized arthropods, e.g. from tiny mites, thrips and aphids, to large planthoppers, heteropterans, dipterans, ticks, and ovipositing hymenopterans. This flexibility will be especially valuable for researchers working on arthropods for which there are few or no previous studies to serve as guidelines. Additionally, new studies such as testing the above hypothesis on AC vs. DC applied voltages (and other research questions) can be quickly and easily performed.

We provide herein the block diagram and basic circuit description of our new AC–DC Correlation Monitor, and begin the study of its applications, by comparing AC- vs. DC-type waveforms produced by this new monitor with a well-known model species, the pea aphid. Future papers will compare AC- vs. DC-type waveforms for leafhoppers and heteropterans.

Our new AC–DC Correlation Monitor combines design features from both the AC Missouri monitor and DC Tjallingii monitor, plus provides new innovations and modernizes the electronics. It can produce up to three simultaneous, parallel, time-synchronized, output signals from a single insect, via both AC and DC signal processing circuitry (a concept first applied in Kindt et al., 2006), using precisely and reproducibly controlled AC-only, DC-only, AC-plus-DC, or 0 V substrate voltage. The new design also includes switchable input resistors, allowing users to tailor the primary circuit's amplifier sensitivity to match the specific emf/R responsiveness spectrum of the recorded insect species (Tjallingii, 1985, 1988; reviewed in Section 4). This feature also allows rapid identification of R vs. emf components, which will help speed waveform characterization and definition for new arthropods. We also herein provide an empirical demonstration of the effect of varying input impedances on aphid waveform fine structure, for the first time for any AC or DC monitor. The present study's research conclusively demonstrates that an AC monitor can be designed to duplicate the level of detail and appearance (i.e. fidelity) of aphid waveforms produced by DC monitors, including all R- and emf-component waveforms.

2. Materials and methods

2.1. Insects and plants

Pea aphids, *Acyrthosiphon pisum* L., were acquired from J. Dillwith, Oklahoma State University, from his clonal colony of

aphids continuously reared on faba bean, *Vicia faba* L. Aphids were greenhouse-reared in Parlier, CA, on faba bean cv. 'Windsor' under supplemental lighting with a photoperiod of 16:8 L:D and temperature ranges of 18–30 °C.

2.2. Waveform recordings

Pea aphids were tethered to gold wire of diameter 25.4 μm (sold as 0.0010 in.; Sigmund Cohn Co., Mt. Vernon, NY, USA) using hand-formulated silver glue (1:1:1 [w:w] of water-based household glue: silver powder: water) provided by W. F. Tjallingii (personal communication, Wageningen Univ., The Netherlands, retired). Aphids were acclimated on host plants for 0.5–4 h following wiring, then starved (while dangling from their wires) for 20 min–3 h before being recorded on a fresh host plant for varying access times from 4 h to 2 d (the wide divergence in time is explained further, below). Waveforms were digitally acquired at a sample rate of 100 Hz, using a WinDaq DI-720 A/D converter and displayed with WinDaq Pro+ software (DATAQ Instruments, Akron, OH, USA) on a Dell notebook computer. After some experimentation, substrate voltages were standardized at 5 mV for AC and 25 mV for DC, for Ri levels of 10^7–10^9 Ω. For Ri 10^6 Ω, AC substrate voltage was raised to 50–75 mV and DC substrate voltage to 50 mV. No substrate voltage (i.e. 0 V) was used for Ri 10^{13} Ω.

All aphid waveform types were analyzed for coarse structure. However, for comparisons of waveform fine structure, emphasis was placed on two model waveform types whose electrical origin is primarily emf, i.e. pd and E2. Two experimental methods were used to test the effects of all possible combinations of Ri level and substrate voltage. First, switches of Ri and substrate voltage settings were made during long durations of pathway activities (i.e. waveforms C, pd) or during passive phloem ingestion (E2) of a single aphid. After each switch was made, gain settings and/or offset voltages were adjusted for optimum display of waveforms; waveforms were then allowed to continue undisturbed until two or three pds or at least 1 min of E2 had occurred, before another switch was made. In this manner, most Ri levels were tested within a single probe for a single aphid. These tests were repeated using additional individual aphids. For the second experimental method, an aphid was allowed to feed unimpeded all night long, with the monitor settings left unchanged, to observe undisturbed waveforms consummating in E2. Waveform appearances were highly consistent, within each Ri-substrate voltage setting, regardless of which experimental method was used, differing only in noise levels caused by quality of wiring. Thus, waveforms in the figures were derived from both experimental methods. A total of 5–10 individual aphids were examined for each Ri-substrate voltage setting and experimental method, for a total of nearly 300 aphids examined. The cleanest, most representative example of each waveform type for each monitor setting was then chosen for figures. In all experiments, two channels were used to simultaneously display waveforms from DC or AC signal processing.

2.3. Monitor designs

Because AC monitors ideally require an AC substrate voltage supplied to the plant, while DC monitors ideally require a DC substrate voltage, the AC–DC Correlation Monitor can supply either AC, DC, both, or neither (i.e. 0 V) to the plant. The signal from the insect then is split into two different (i.e. AC and DC) signal processing circuits, similar to what was proposed by Backus et al. (2000) and Tjallingii (2000).

The AC–DC Correlation Monitor also has four additional features not proposed in the Walker and Backus (2000) chapters: (1) a third AC channel that can be switched to the Missouri monitor v. 2.2 design (Backus et al., 2000), via a coupling capacitor, for comparison with waveforms published from studies using this monitor; (2) a log amplifier, to compress high voltage signals from very large insects like certain heteropterans; (3) an offset knob, which shifts the signal voltage level prior to rectification of AC signals, in order to maintain waveform fidelity with DC output, and (4) the most significant design innovation of all, i.e. multiple, switchable input resistors of 10^6, 10^7, 10^8, 10^9 and 10^{13} Ω (the latter is similar to the "emf-only" amplifier of the Tjallingii DC monitor; Tjallingii, 1985, 1988). These innovations allow dynamic comparison of waveform appearances from different electronic circuits.

2.4. General circuit description

Fig. 1 shows the block diagram of the AC–DC Correlation Monitor. Circuit descriptions will emphasize a comparison between the new design and that of the Missouri monitor (Backus and Bennett, 1992; Backus et al., 2000) or the Tjallingii DC monitor.

2.4.1. Oscillator–substrate output circuit (Fig. 1, left box)

The AC–DC Correlation Monitor begins operation by generating AC and/or DC substrate voltages. The AC oscillator generates an accurately set 1 V RMS signal, which is applied to the AC substrate voltage (level) control. Similarly, the DC selector switch sends an accurate +/−1 V DC signal from the power supply to the DC substrate voltage control. A single, 1000 Hz frequency, is now used instead of the multiple frequencies (continuously variable 100–10,000 Hz) in the Missouri monitor (Backus and Bennett, 1992; all versions). This fixed frequency was chosen to afford excellent waveform resolution and noise blockage, as well as the most practical compromise for demodulation of the signal, while avoiding capacitive effects. AC and DC voltages in the range of 0–1000 mV can be precisely and reproducibly set and applied to the plant, either separately or mixed together. Output voltage is a composite of the DC level and the AC carrier wave. In effect, the AC sine wave's horizontal axis of symmetry is moved up or down by adding (for positive) or subtracting (for negative) the DC voltage, as an offset. The voltage supply circuits are in a box that is kept outside of the Faraday cage in which the insect and plant preparation are located.

2.4.2. Head stage amplifier (Fig. 1, middle)

Adopting an excellent feature first used in the DC (Tjallingii) system, the design now incorporates an external head stage amplifier for the first amplifier in the chain (i.e. the amplifier in the primary circuit; Backus et al., 2000; Walker, 2000) (Fig. 1). The head stage amplifier is placed inside the Faraday cage, thus allowing better noise control because (1) it isolates the amplifier from the power supply in the oscillator, outside the cage, and (2) the signal from the head stage amplifier is generated in close proximity to the experimental preparation (i.e. insect on plant). The minimal length of conductor cable between the amplifier input and the insect eliminates signal attenuation from capacitive loading effects (i.e. frequency-variable loss of signal amplitude, leading to distortion of waveform shape). This design preserves waveform fidelity better than did any version of the Missouri monitor (v. 1.0, Backus and Bennett, 1992, or v. 2.2, Backus et al., 2000). The head stage amplifier also provides gain, i.e. becomes an active signal source capable of driving an undistorted signal through the length of coaxial cable. The insect signal is amplified by adjustable gain in the head stage amplifier.

A knob on the head stage amplifier allows the user to select input resistor (Ri) level among 10^6, 10^7, 10^8, or 10^9 Ω (therefore providing a mixture of emf and R components in the signal; see details on emf/R responsiveness curves and inherent resistance in Section 4) or 10^{13} Ω (the inherent resistance of the amplifier, for

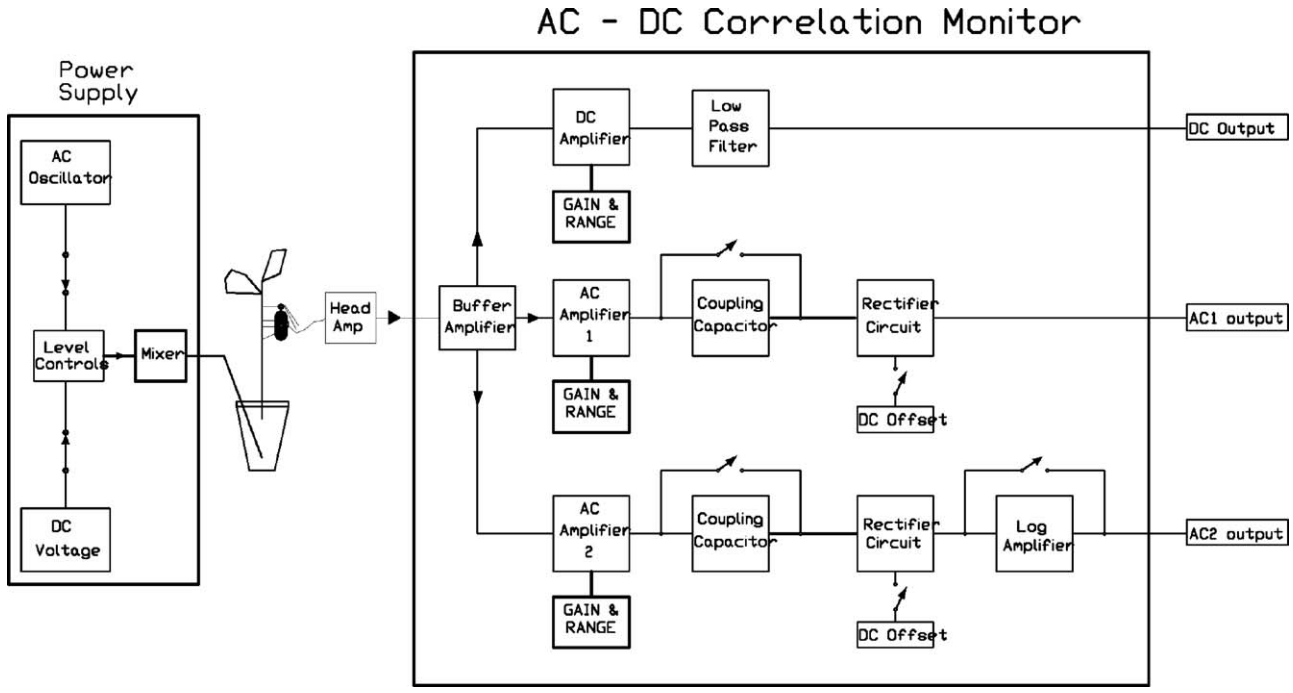

Fig. 1. Block diagram for the new AC–DC Correlation Monitor.

recording emf only). The selected input impedance may be changed at any time during the experiment.

2.4.3. Input buffer amplifier (Fig. 1, right box)

The input buffer is the first amplifier inside the main box of the instrument, which also is placed inside the Faraday cage, again for noise isolation. The buffer amplifier insures that the signal from the head stage amplifier is unchanged in amplitude and appearance at the inputs of all three parallel, downstream signal-processing amplifier chains (Fig. 1). Its small gain also compensates for any signal loss that might have occurred in the coaxial cable between the head amplifier and the three signal processing circuits (Fig. 1).

2.4.4. DC amplifier (Fig. 1, right box, top row)

The DC signal processing circuit in the AC–DC monitor is more elaborate than that used in the DC (Tjallingii) system, because AC voltages must be removed from the signal. Thus, for the DC channel, we use a gain stage similar to the Tjallingii monitor followed by an active, lowpass filter to remove any lingering AC from the signal (Fig. 1). The filter begins to delete AC signal components above 80 Hz, significantly above the maximum frequency of aphid waveforms for EPG [see discussion in Tjallingii, 2000; Backus et al., 2000]). Total attenuation at 1000 Hz is just over seven orders of magnitude, or ten million times; thus, providing very strong elimination of AC from the DC signal processing.

2.4.5. AC amplifiers (Fig. 1, right box, middle and bottom rows)

The AC–DC Correlation Monitor is designed, in part, to explain differences and similarities between DC and various AC EPG signals from past monitor designs. Thus, we provide two, parallel AC amplifier chains in separate channels in the monitor (Fig. 1). This allows the user to dynamically compare the effects of design features such as the interstage coupling capacitors and logarithmic amplifier that were found in past monitor designs. Otherwise, the major part of each AC amplifier chain is very similar to the Missouri monitor (v. 1.0, Backus and Bennett, 1992, v. 2.2, Backus et al., 2000). The possible gain range of the instrument is 0–10,000 (including the head stage amplifier's gain of 100×). This large gain range affords great flexibility in gain to the AC–DC Correlation Monitor. Unless there are insurmountable noise issues, even the tiniest to largest arthropods should be recordable using some combination of Ri and gain.

Until recently, operational amplifiers had internal arrangements that caused an artifactual DC signal component (i.e. an increase or decrease in voltage level) in the form of a gradual baseline drift that was superimposed onto the output signal-of-interest, thus incorporated into the final waveform. DC interstage blocking (or coupling) capacitors between amplifier stages eliminated this artifactual drift. Coupling capacitors were standard design features in the 1980s and 1990s; three coupling capacitors were included in both versions of the Missouri monitor (Backus and Bennett, 1992; Backus et al., 2000). More modern operational amplifiers, such as the ones used in the present design, have made this offset error so tiny that the capacitors are no longer necessary. Thus, the AC–DC Correlation Monitor uses operational amplifiers that are functionally superior to those used in all previous designs, including the Missouri AC monitor and Tjallingii DC monitor. This probably explains why the AC–DC Correlation Monitor, unlike, e.g. the Tjallingii DC monitor, does not display drift in the voltage level of the output signal over time.

To demonstrate the absence of baseline drift in the present design's output, three test aphids were recorded for up to 75 continuous hours using the AC–DC Correlation Monitor set at (true) 0 V substrate voltage. For that entire time period, the output voltage level of the baseline (non-probing) waveforms in the DC signal processing channel changed by less than 2 mV, after maximum amplification. Therefore, the unamplified change would have been on the order of nanovolts, far less voltage change than is routinely seen over such a time span in DC monitor recordings. Although the quality of the aphids' wire connections deteriorated in those 75 h, with consequent reductions in waveform amplitude and resolution, there was still no baseline drift in the present design's output. Therefore, we hypothesize that amplifier artifacts are the actual source of baseline drift in the DC Tjallingii monitor design, whose type of amplifiers are notorious for such artifacts. Baseline drift in that DC monitor's output, combined with imprecise substrate voltage control knobs, cause lack of reproducibility of substrate voltage levels; they cannot be established for

an experiment, but require adjustment for each new recording (Kindt et al., 2006). Our design now corrects this unnecessary experimental issue.

Although coupling capacitors can solve problems with voltage artifacts, at the time that the Missouri AC monitor was designed we did not anticipate that coupling capacitors might negatively impact waveform appearance. However, coupling capacitors remove DC components in the signal, i.e. rapid changes in voltage level, such as occur at the beginning and end of the aphid pd (sub-phases I and III, respectively). Thus, these pd sub-phases (and other rapidly changing waveforms) could be severely distorted by coupling capacitors. Accordingly, for empirical comparisons with Missouri monitor published waveforms, both AC channels of our AC–DC Correlation Monitor were equipped with a switchable coupling capacitor (Fig. 1). To demonstrate the coupling capacitor's effect on waveform output, two preliminary tests were performed with a prototype AC–DC Correlation Monitor in which one AC channel was installed with a Missouri monitor v. 2.2-type amplifier (hereafter, AC 2.2) and fixed coupling capacitors. Output from this channel was compared with those from the AC and DC signal processing channels (called AC 3.0 and DC for this experiment, respectively, below) using the new type of amplifier with switchable coupling capacitors. Results (described in the next section) of these comparison tests were used to optimize the present monitor design described herein.

2.4.6. Rectifier (Fig. 1, left box, middle and bottom rows)

Both AC channels in the AC–DC Correlation Monitor use a precision full-wave rectifier to remove the AC carrier wave from the signal in the final output, similar to the one in the Missouri monitor (Backus and Bennett, 1992). The present rectifier circuit design provides a compromise between absolute removal of carrier remnant (explained in Backus et al., 2000) vs. perfect reproduction of relatively high-frequency signal components from the insect. Interestingly, this circuit effectively has no cut-off frequency. The 1 μF filter capacitor averages the AC carrier amplitude and accurately follows the modulated carrier in "drawing the envelope" (Backus and Bennett, 1992). Therefore, the rectifier removes the carrier wave perfectly and accurately (with no distortion) down to pure DC (0 Hz). Any combination of AC-plus-DC signal components will be faithfully reproduced by the circuit. Thus, we herein correct an error in the circuit analysis of Backus et al. (2000) and Tjallingii (2000), wherein a cut-off frequency of 0.8 Hz for this rectifier's supposed lowpass filter was mistakenly cited. The actual absence of a cut-off frequency in the rectifier, in combination with higher Ri levels and the absence of coupling capacitors or filters, probably account for the high fidelity of emf-component waveforms in the AC–DC Correlation Monitor.

The DC offset control associated with the rectifier (Fig. 1) is a new feature of the AC–DC Correlation Monitor not present in the Backus and Bennett (1992) circuit for the Missouri monitor. It eliminates an interesting waveform artifact caused by the precision rectifier. In the absence of a coupling capacitor (i.e. if it is switched out in the present design), the AC amplifier becomes fully sensitive to DC components in the signal. Thus, aphid pd sub-phases I (the drop) and III (the rise), will be retained. However, when this retained DC voltage level crosses the horizontal axis of symmetry of the rectifier (i.e. 0 V), it will be inverted by the subsequent action of the full-wave rectifier. The aphid pd crosses this axis as it goes from positive to negative voltage level. Thus, the portions of the pd that reside below 0 V (i.e. sub-phase II and its parts) will become inverted (mirror-imaged) to positive-going by the rectifier, while positive-going portions will remain unaffected. To correct this problem for below-0 V signals passing through the AC amplifier, the DC offset voltage control is included to introduce a positive or negative voltage to the signal after the measuring point. Thus, the insect does not experience this voltage. A positive offset voltage allows the user to shift the whole waveform upwards, until all portions are positive, or above the axis of symmetry, before rectification. Using the offset knob will avoid inversion of negative-going signal components. This will preserve absolute waveform fidelity for a signal undergoing AC signal processing with that of the same signal undergoing DC processing. For newly recorded species, the offset may be used experimentally to determine whether a portion of the AC amplifier's output is affected by the rectifier, and therefore more correctly should be portrayed as negative-going. The latter can be easily identified by comparing the AC and DC outputs, and adjusting the offset voltage level until the two look identical. This process can quickly identify signals that are due to negative-going emf components.

Results of the AC 2.2 vs. AC 3.0 comparisons demonstrate the effects of both the coupling capacitors and the offset voltage

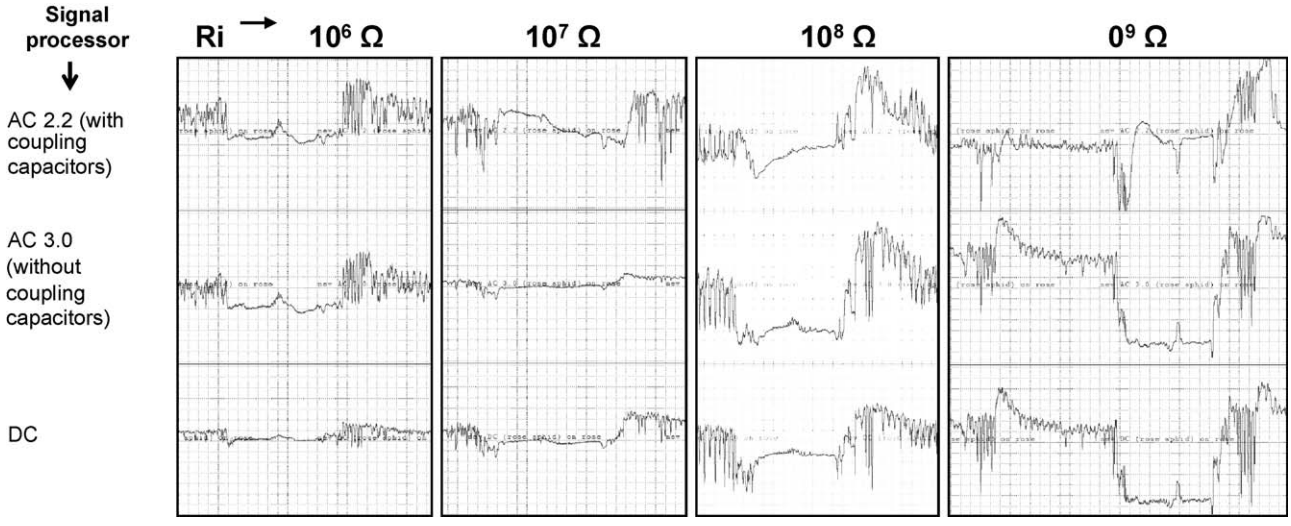

Fig. 2. Pea aphid waveform excerpts showing C-pd-C waveforms using AC substrate voltage. The three waveform excerpts in each column are simultaneous recordings of the same insect with different signal processing. Each column is from a different C-pd-C sequence. Top row: AC 2.2 amplifier (see text) with fixed coupling capacitors present; middle row: AC 3.0 channel with coupling capacitors switched off; bottom row: DC 3.0 channel, for each of four input resistor (Ri) levels from 10^6 to 10^9 Ω (columns). Small offset voltage was used on both AC channels (see text). Aphid pd sub-phase II waveforms are inverted in AC 2.2 channel (top) at Ri 10^9 Ω. All waveforms are at Windaq compression 5 (1.0 s/div), Windaq gain 16× or 32×.

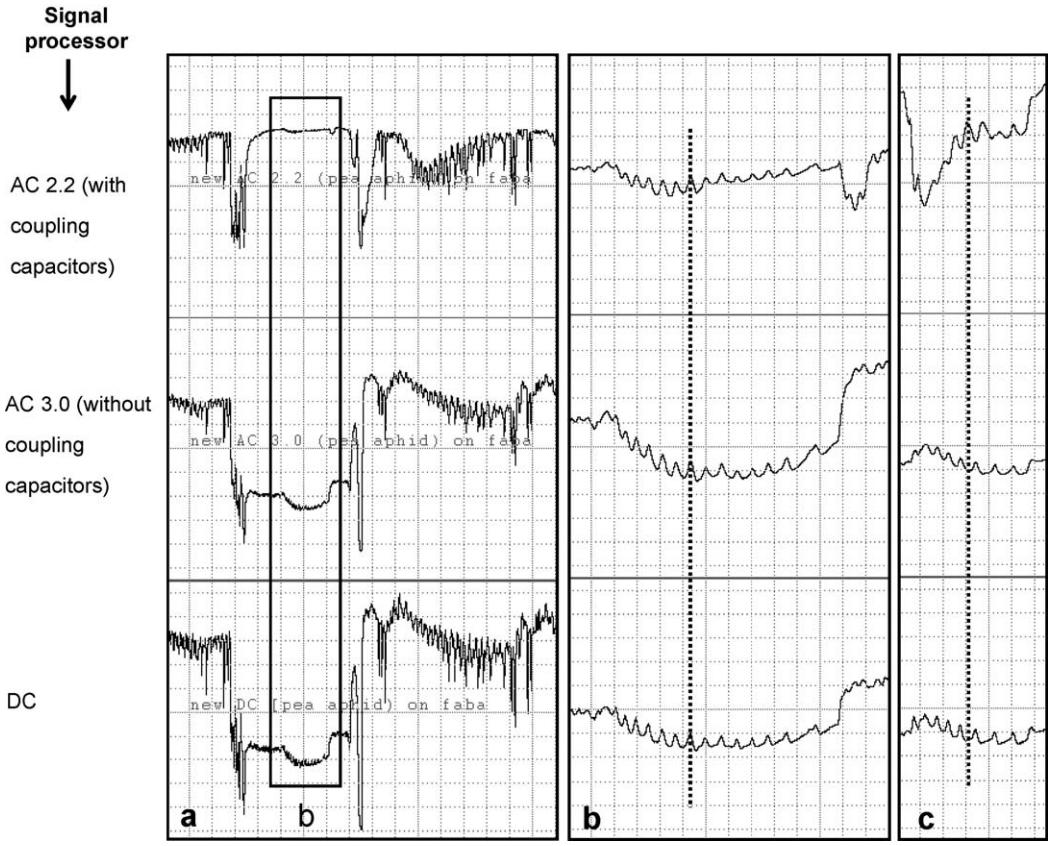

Fig. 3. Pea aphid waveform excerpts showing C-pd-C waveforms using AC-plus-DC substrate voltage. The three excerpts in each column are as in Fig. 2, except only Ri $10^9\ \Omega$ was used, with large offset voltage unless otherwise stated. (a) C-pd-C excerpt at Windaq compression 5 (1.0 s/div), Windaq gain 16× (top) or 32× (middle and bottom). (b) Enlarged view of sub-phase II waveforms from box b in part a. Windaq compression 1 (0.2 s/div), Windaq gain 64× (top), 128× (middle and bottom). AC 2.2 (top) had coupling capacitors present with large offset, showing no rectifier fold-over. AC 3.0 (middle) had no coupling capacitors with large offset, also showing no rectifier fold-over. Dotted line shows that all fine-structure peaks line up with peaks; therefore the waveform in the top row is elevated, not inverted. (c) Enlarged view from later in the same recording, with same Windaq compression and gain levels as part (b). Offset was removed from the AC 2.2 channel; therefore rectifier fold-over and inversion occurred. Dotted line shows that peak in top row lines up with valleys in middle and bottom rows; therefore the waveform in top row is inverted. Pale gray lettering is user annotation verifying channel identity.

control. In electronic circuit design, the express function of coupling capacitors is to remove voltage offsets. Thus, if the signal-of-interest is simple, like a low-frequency sine wave, the two types of devices can cancel out one another's effects. However, EPG waveforms are not simple, and our empirical comparisons showed that there were slight but important differences in these device's effects on output waveforms. Excerpts of C-pd-C events during pathway are shown in the first comparison test's results (Fig. 2). Each waveform excerpt is recorded simultaneously in each of the three (prototype) signal processing displays (i.e. AC 2.2 [top row], AC 3.0 [middle row] and DC [bottom row]) for each Ri level selected (i.e. each figure column). A very small offset voltage was applied to both AC channels (this prototype monitor had only one quarter the offset voltage capability of the present design). At most Ri levels (10^6–$10^8\ \Omega$ Ri), the rectifier did not cause waveform inversion because the pd did not drop below 0 V at those Ri levels. Coupling capacitors (present in the AC 2.2 channel vs. absent in the AC 3.0 channel) caused some elevation of the pd waveform, especially at 10^7 and $10^8\ \Omega$ Ri levels, but the middle section of the pd (sub-phase II) was not inverted. However, a mirror-image distortion occurred at $10^9\ \Omega$ Ri, because the pd abruptly fell below 0 V at that Ri level. The pd sub-phase II waveforms were moved into the positive voltage range by the AC 2.2 circuit and inverted in the process (Fig. 2, top row; see prominent peak pointed downward instead of upward). Thus, some, but not all, DC information was lost. The rectifier caused fold-over and inversion of the pd, while the coupling capacitor caused severe distortion of the sub-phases I and III drop and rise (Fig. 2). At $10^9\ \Omega$ Ri, the small offset was sufficient to prevent rectifier fold-over of the pd in the AC 3.0 channel, but not in the AC 2.2 channel.

The AC 3.0 and DC channel outputs otherwise are virtually identical in Fig. 2, but the AC 2.2 output shows slight differences in the appearance of the pathway (C) waveforms from the other two outputs at Ri 10^8 and $10^9\ \Omega$ (although gain at some Ri levels was not yet sufficient in this early prototype, making certain comparisons challenging). The C waveform differences in Fig. 2 are probably due to amplifier resolution levels, because neither the actions of the coupling capacitors nor the offset voltage should affect waveform resolution.

In a second comparison test performed after the prototype monitor's gains and offset voltage levels were increased, similar waveform outputs were used to examine more closely the rectifier's inversion vs. the coupling capacitor's elevation effects. Using AC-plus-DC substrate voltage, and solely $10^9\ \Omega$ Ri, Fig. 3a shows the usefulness of a large offset voltage (applied to both AC channels) in avoiding the rectifier fold-over in the AC 3.0 channel (i.e. in absence of coupling capacitors). Its pd is virtually identical to that in the DC channel (taking into consideration slight amplification differences between channels). However, because of the large offset, the presence of the coupling capacitors in the AC 2.2 channel caused elevation, not inversion, of the pd sub-phase II waveforms (see the amplified and expanded views in Fig. 3b). Thus, the capacitor's individual effect could be identified because the offset voltage was sufficient to avoid rectifier fold-over. The offset

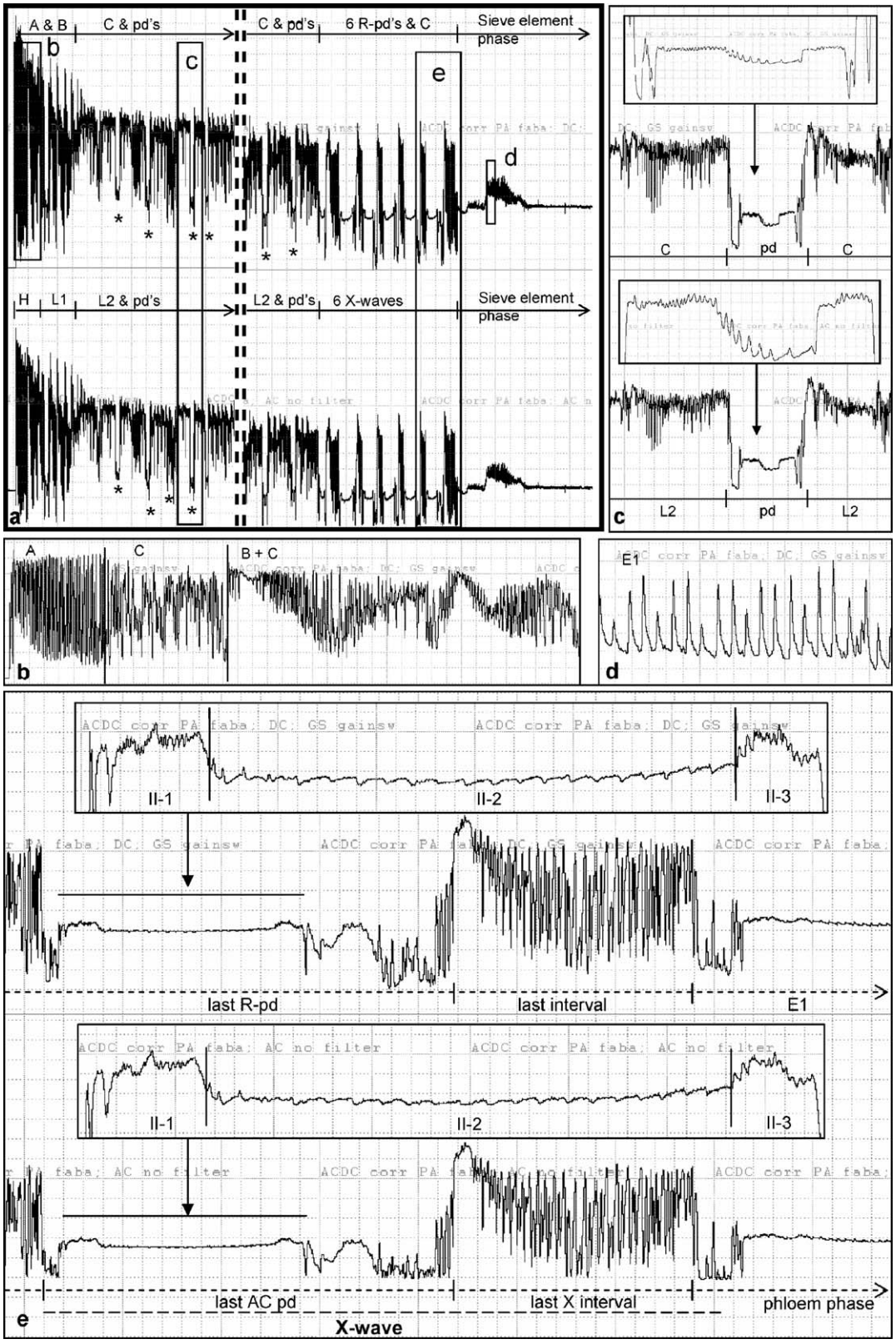

Fig. 4. (a) (Bolded boxes, upper left) Compressed pea aphid waveform output at Ri 10^9 Ω, from the DC signal processing channel (top row, with DC waveform labels) and the AC signal processing channel (bottom row, with AC waveform labels). Left bold box shows the beginning of the probe; right bold box shows late pathway pds (including X waves) and sieve element phase. Windaq compression level 100 (20 s/div), Windaq gain 16× or 32× unless otherwise noted. (b) Expanded DC channel waveforms in box b from part a, showing waveform types A and B separated by vertical line. Windaq compression level 7 (1.4 s/div). (c) Expanded AC and DC channel waveforms in box c from part a, showing waveform types C and pd (DC terminology) or L2 and pd (AC terminology). Windaq compression level 7 (1.4 s/div). Inset boxes are at Windaq compression 1 (0.2 s/div); top box at Windq gain 16×, bottom box at Windaq gain 64×. (d) Expanded DC channel waveform E1 in box d from part a. Windaq compression 2 (0.4 s/div). Pale gray lettering is user annotation verifying channel identity. (e) Expanded AC and DC channels from box e in Fig. 4a, showing components of X-wave (pd and interval) with DC-type labeling on DC channel (top row) and AC-type labeling on AC channel (bottom row). Windaq compression 5 (1.0 s/div), Windaq gain 8×. Inset boxes show main part of pd more expanded, labeled with pd sub-phase numbers. Windaq compression 2 (0.4 s/div), Windaq gain 16× or 32×. Pale gray lettering is user annotation verifying channel identity.

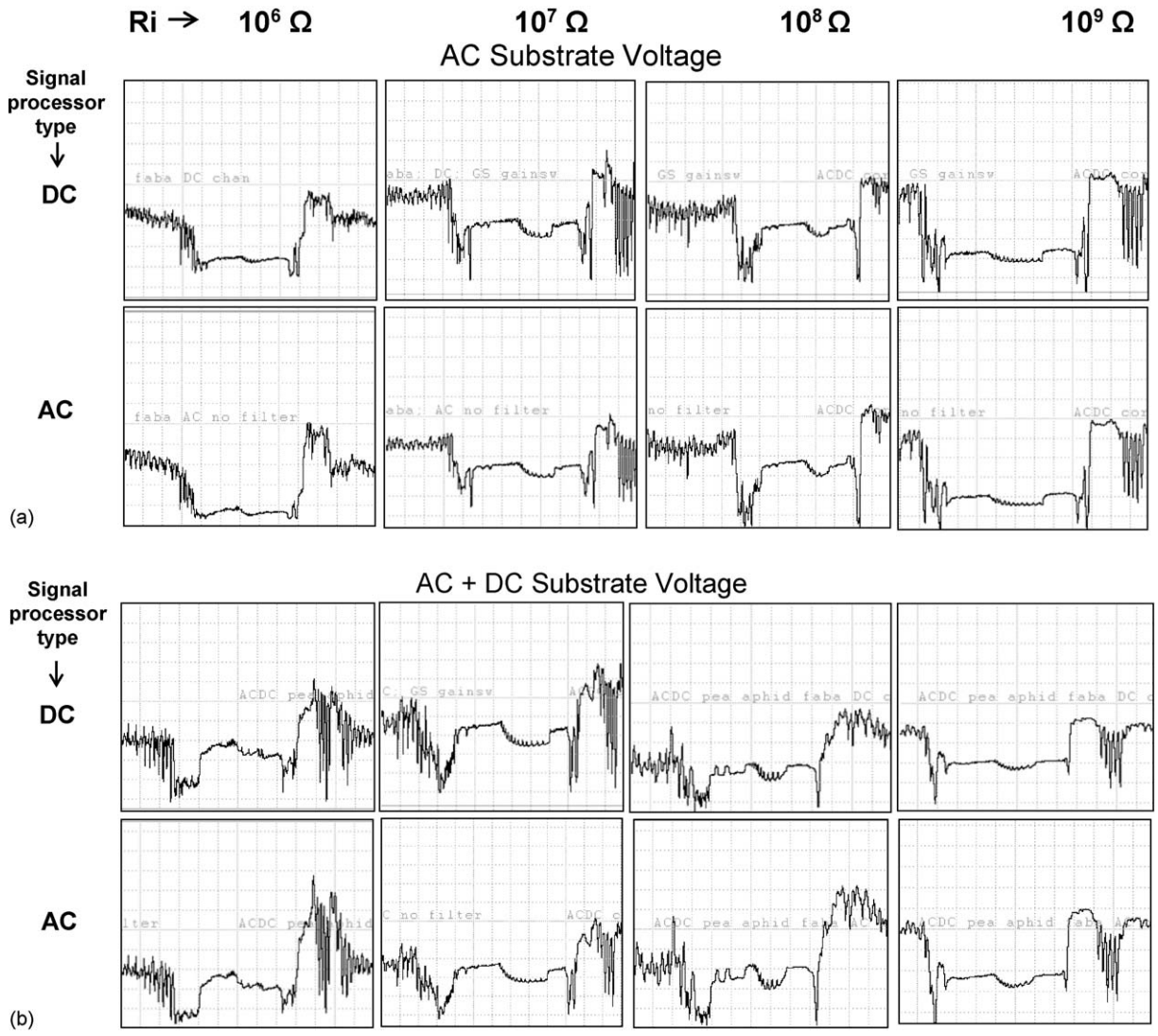

Fig. 5. (a) Pea aphid waveform excerpts showing C-pd-C waveforms using AC substrate voltage. The two waveform excerpts in each column are simultaneous recordings of the same insect with different signal processing. Each column is from a different C-pd-C sequence. Top row: DC signal processing, bottom row: AC signal processing. The AC channel had coupling capacitors switched off, and offset voltage used to remove rectifier fold-over of AC channel. Each column is from a different C-pd-C excerpt, for each of four input resistor (Ri) levels from 10^6 to 10^9 Ω (columns). All waveforms are at Windaq compression level 5 (1.0 s/div), Windaq gain steps 16× or 32×. (b) Same for AC-plus-DC substrate voltage.

was then removed for another pd in the same probe. Rectifier fold-over occurred in the AC 2.2 channel to give the inverted, mirror-image view of the sub-phase II fine structure (Fig. 3c, showing only the enlarged view), The coupling capacitors in the AC 2.2 channel enhanced the distortion caused by the fold-over. With offset present and coupling capacitors switched out, the AC 3.0 channel again was virtually identical to the DC channel (Fig. 3c).

These tests show that the effects of coupling capacitors and rectifiers on EPG waveform fine structure can differ slightly for waveforms below 0 V. Coupling capacitors cause elevation of the signal, while rectifiers cause inversion (mirror-imaging). Both types of effects can interact as they move the waveform into the positive range. Thus, to retain complete waveform fidelity with published DC aphid waveforms at Ri 10^9 Ω, an AC monitor circuit must have large offset capability without coupling capacitors.

2.4.7. Logarithmic amplifier (Fig. 1, left box, bottom rows)

One AC amplifier channel also incorporates a logarithmic amplifier to provide amplitude compression of the highest amplitude signals. This circuit is designed for recordings of large insects with good conductivity that might show large signal excursions, yet with low-voltage fine structure that provides relevant biological information. Thus, it amplifies the fine structure while still retaining the ability to reproduce the highest waveform peaks. This is similar in concept to the logarithmic filter of Kawabe et al. (1981); thus it can also be used to replicate waveforms published therein and elsewhere.

3. Results

Taking into consideration differences due to wiring quality, both coarse and fine structure appearances of aphid waveforms were highly consistent among individual insects, for each combination of input impedance (Ri level) and substrate voltage type.

3.1. Waveform Overview at Ri 10^9 Ω

A compressed overview of a pea aphid probe (pathway plus early sieve element phase), recorded at Ri of 10^9 Ω with an AC substrate voltage, is shown in Fig. 4a (bold box in upper left). This compression level is similar to typical AC waveform displays in the

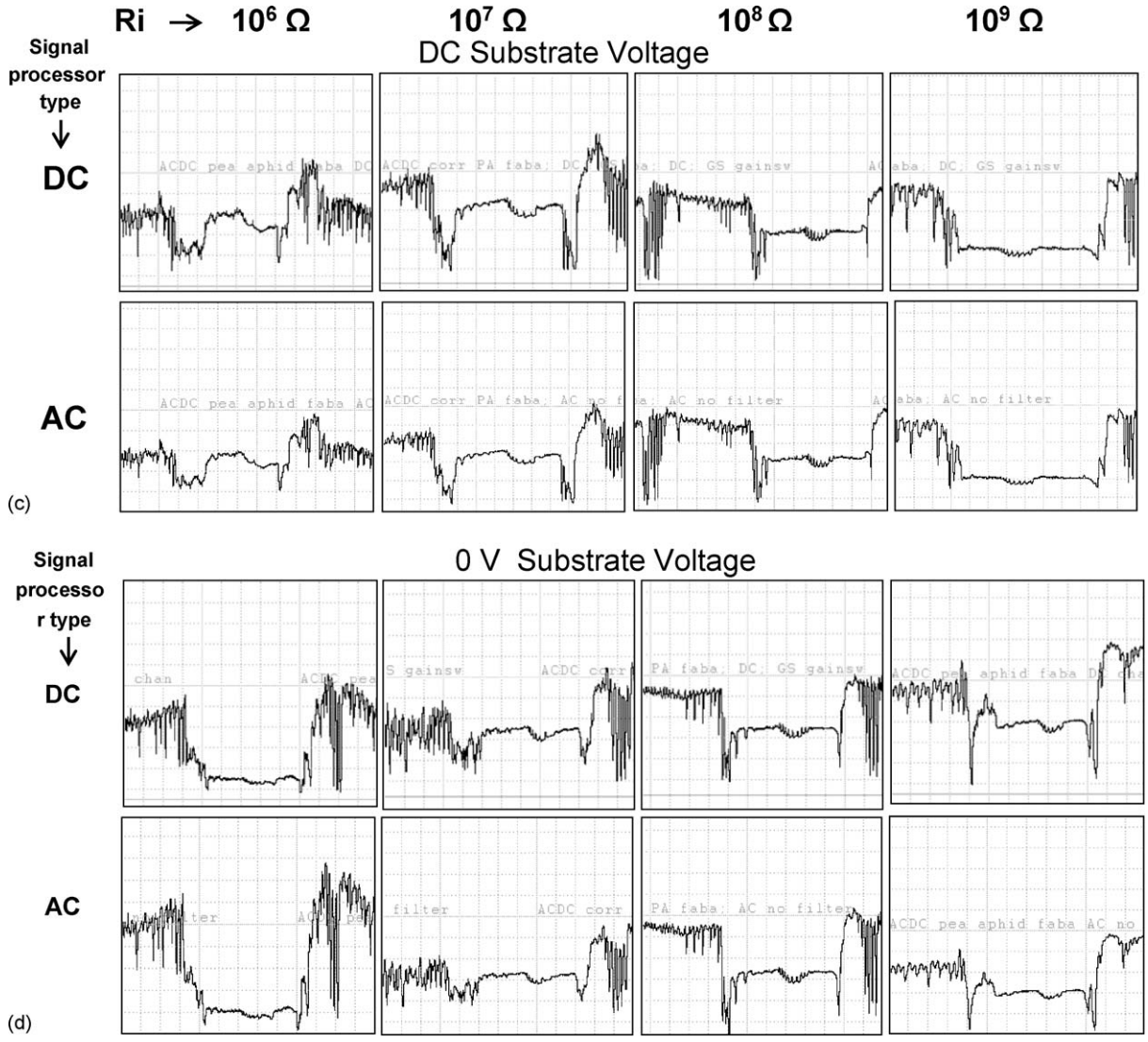

Fig. 5. More pea aphid C-pd-C excerpts. (c) Same for DC substrate voltage. (d) Same for 0 V substrate voltage. Pale gray lettering is user annotation verifying channel identity.

past, and all of the waveforms bear a striking resemblance to the diagram of AC aphid waveforms in Backus (1994), with slight differences described further below. It is apparent from comparing the upper waveform trace (recorded with DC signal processing, and labeled with DC waveform names) with the lower trace (recorded with AC signal processing, and labeled with AC names), that the compressed outputs are virtually identical at this coarse-structure level. Figs. 4b–e (and all other figures) illustrate expanded, more detailed views of the major aphid waveform types.

3.2. Pathway phase waveforms (A, B, C and pd)

Fig. 4b shows an expanded view of the box labeled 'b' in Fig. 4a (from DC signal processing), which illustrates that the pathway waveforms A, B and C are distinguishable and resemble published views of DC waveforms at Ri $10^9\ \Omega$ (Tjallingii, 1995). Likewise, Fig. 4c shows an expanded view of the box labeled 'c' in Fig. 3a (from both AC and DC signal processing), an early-pathway pd with sections of waveform C or L2 before and after. As shown in the inset boxes above each waveform trace in Fig. 4c, fine structure of the pd is nearly identical for both AC and DC signal processing (Fig. 4c, insets; amplified slightly more in the lower inset; therefore differences are due to gain). The three sub-phases of the lower pd (II-1, II-2, and II-3; Fereres and Collar, 2001) are recognizable, and very similar in appearance to published versions of normal pds for pea aphids (Tjallingii and Gabrys, 1999).

In a similar manner, C-pd-C waveform excerpts recorded with different Ri levels and substrate voltage types are displayed as a collage in Fig. 5a–d. Appearances of pds within each Ri level (column) and substrate voltage (outer boxes) are virtually identical to one another, when compared for the AC and DC signal processing channels for all four substrate voltage types (taking into consideration slight differences in amplification among channels). Thus, for pathway-type, R-plus-emf waveforms considered *within each input resistor level*, there was no difference in waveform output appearance between AC and DC signal processing in the AC–DC Correlation Monitor.

There were, however, significant differences in the appearance of the pd among Ri levels. These differences sometimes interacted with substrate voltage type used. At Ri $10^6\ \Omega$, the pd waveform dropped slightly and then quickly rose again, forming a depressed hump with AC-plus-DC substrate voltage (Fig. 5b) and DC-only (Fig. 5c). In contrast, with AC-only (Fig. 5a) and 0 V (Fig. 5d), the pd appearance was a flat line. These features interrupted the otherwise higher-frequency, repetitive pattern of the C waveform. Thus, while the $10^6\ \Omega$ pds of the AC and 0 V substrate voltages were flatter than those with AC-plus-DC or DC only, they were still distinguishable from the C waveform. At Ri 10^7 and $10^8\ \Omega$, all of the

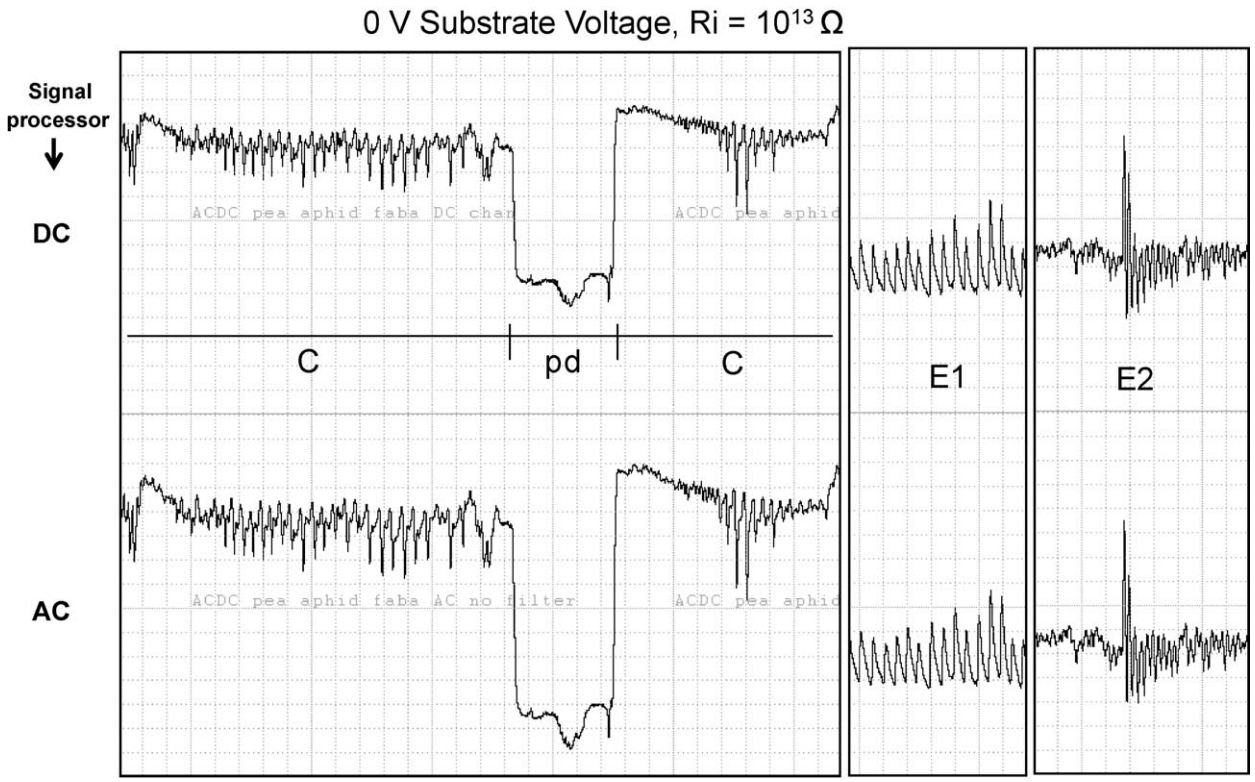

Fig. 6. Waveforms from pea aphid recording at Ri 10^{13} Ω. Top row: output from DC signal processing, bottom row: output from AC signal processing. Left column, C-pd-C, middle column, E1; right column, E2 showing waves and spikes but little or no peaks. All are at Windaq compression 5 (1.0 s/div), Windaq gain 8× for DC, 4× for AC. Pale gray lettering is user annotation verifying channel identity.

pd waveforms resembled similar, depressed humps, but occurred at a higher voltage level with more distinctly recognizable details than at 10^6 Ω. At Ri 10^9 Ω, the voltage level of the pd became shifted to the negative. Also, the 0 V depressed hump of the DC pd was accentuated by deeper drops-and-returns at the beginning and end, while the AC pd was less accentuated and the hump was flatter. Pds from AC-plus-DC substrate voltage (Fig. 5b) resembled those from AC voltage (Fig. 5a) more than from DC voltage (Fig. 5c). The DC-only pd sank lower than pathway level and remained low at Ri 10^9 Ω (similar to the Tjallingii DC monitor output). Consequently, output waveform appearances were similar at lower Ri levels when either AC substrate voltage or no substrate voltage of any type was applied (0 V; therefore the only voltage driving the R component was the electrode potential; Fig. 4d). The higher the Ri level and more DC present in the substrate voltage (i.e. AC-plus-DC or DC only), the more the output resembled that of the Tjallingii DC monitor.

When Ri level was switched to 10^{13} Ω (emf only), the pd dropped even more strongly negative (Fig. 6), using both AC and DC signal processing. The pd sub-phases were present but less distinct, very similar to those seen for "pure emf" recordings in the DC literature.

3.3. X waves (R-pds)

An expanded view of the final X wave (in AC terminology), or final R-pd-plus-interval (in DC terminology; Tjallingii and Gabrys, 1999), is shown for Ri 10^9 Ω (AC substrate voltage) in Fig. 4e. Again, the waveform output from the DC (top row) and AC (bottom row) signal processing channels were virtually identical to one another, and almost identical to published pea aphid waveforms (Tjallingii and Gabrys, 1999). All three sub-phases of the R-pd were distinguishable (inset boxes, labeled), differing only slightly in appearance from the published versions. X waves/R-pds were also seen frequently at the other Ri levels with all substrate voltages, and their resemblance to the one portrayed was very strong. Slight differences by Ri level paralleled those of pds across Ri levels (Fig. 5).

3.4. Sieve element ingestion waveform (E2)

The appearances of the E2 waveform at different Ri values and substrate voltage types (Fig. 7) were also compared. As with the C-pd-C excerpts described above, there were almost no differences between AC and DC signal processing channels, within each Ri level for each substrate voltage (Fig. 7). The exception occurred at Ri 10^6 Ω for the DC signal processing channel (for all substrate voltages), which showed an amplitude decrease that could not be improved, compared with the AC channel (Fig. 7). It is unknown whether this may be a minor gain problem with the present monitor design that could be changed in future designs.

Comparing E2 waveform appearances among Ri levels and substrate voltage types for either DC or AC channels (Fig. 7) revealed even greater differences than observed for the C-pd-C excerpts, discussed above. There were three main components of the pea aphid E2 waveform, all documented in the recent DC EPG literature (Tjallingii and Gabrys, 1999; Tjallingii, 2000), i.e. monophasic peaks (at a variable repetition rate) and waves (the latter at a uniform 9 Hz repetition rate in our recordings), as well as biphasic, intermittently interrupting spikes (not discussed, but pictured in Tjallingii and Gabrys, 1999) (Fig. 7a, labels). At Ri 10^9 Ω, waves and spikes were present with all substrate voltages. However, peaks were only present when substrate voltage was used (i.e. not with 0 V), and their size varied with type of substrate voltage. They were most prominent with DC-only voltage, small in size with AC-only, and intermediate with AC-plus-DC. It is unclear why peaks were absent at 0 V, when they have been noted in the DC literature when 0 V is applied. Perhaps peaks in the literature

were generated by accidental application of unmeasureable voltage. The 0 V setting on the DC Tjallingii monitor is uncertain, whereas the AC–DC Correlation Monitor can be reliably set at true 0 V. At both Ri 10^7 and $10^8\ \Omega$, all three components (i.e. peaks, waves and spikes) were present using all types of substrate voltages. The greatest diversity occurred at Ri $10^6\ \Omega$. Waves were present with all substrate voltage types; peaks were present whenever DC substrate voltage was used (i.e. DC-only or AC-plus-DC), and spikes were present when AC signal processing was used, regardless of substrate voltage. Tiny spikes were barely visible with DC signal processing, but totally absent when AC-plus-DC substrate voltage was combined with DC signal processing.

3.5. Summary of aphid waveform appearances

Both AC and DC signal processing channels produced waveforms similar to one another and to AC-type waveforms of the Missouri AC monitor (i.e. recorded at Ri $10^6\ \Omega$) when high-resolution, computerized recording was used (Backus, unpublished data). Conversely, waveforms similar to DC-type waveforms were produced via both signal processing channels at Ri $10^9\ \Omega$, again when high-resolution recording was used (Backus, unpublished data). Intermediate input resistor levels showed intermediate waveform appearances.

4. Discussion

4.1. Why is not our AC channel an "optimized AM device"?

Prototype versions of our AC–DC Correlation Monitor included one AC channel with a switchable highpass filter, in an attempt to follow the recommendations of Tjallingii (2000) for an "optimized AM (amplitude modulation) device." In theory, a highly filtered AC channel would detect only R components, by retaining only those signals that modulate the carrier wave (Tjallingii, 2000). Thus, one could achieve the potentially useful goal of a pure R-component output that could be dynamically compared with simultaneous R-plus-emf output. Yet, output from our AM-AC channel was not as expected, and we now believe that Tjallingii's partial success (Kindt et al., 2006) was an artifact of his design and choice of insect subject.

Tjallingii applied his AC–DC monitor to study thrips feeding (Kindt et al., 2006). No details of the design were presented. However, some features can be surmised by combining the suggestions in Tjallingii (2000) with the brief description in Kindt et al. (2006). The monitor supplied an adjustable DC substrate voltage with a superimposed, fixed 800 mV AC substrate voltage of 891 Hz (carrier frequency). After input buffering, the signal was split into simultaneous AC and DC signal processing channels; the AC channel was bandpass- or highpass-filtered at very near the frequency of the carrier wave, then rectified and lowpass-filtered. Unfortunately, no information is provided about the quality or degree of frequency attenuation for this filter.

Our prototype monitor's highpass filter began to attenuate frequencies at just under 1000 Hz (the carrier frequency) and reduced them by a factor of 10,000,000 when the applied frequency dropped to 80 Hz (the Nyquist threshold for theoretical aphid waveforms; Backus et al., 2000). Thus, our filter was deliberately designed to be as close as modern analog electronics allows to a "brickwall" filter that should reduce unwanted frequencies to near zero. However, it relied upon the variable substrate voltages chosen by the user, which (in our experiments) were much lower than 800 mV. These voltages were chosen to minimize exposure to potentially damaging voltage levels. Large insects, especially those with inherent resistances lower than $10^9\ \Omega$, develop higher current densities in their bodies at lower monitor Ri levels than do very small insects like thrips. Very large insects have shown increased irritability under such circumstances (Backus, unpublished data). Insects as tiny as thrips can tolerate high substrate voltages at Ri $10^9\ \Omega$.

Surprisingly, pea aphid waveforms from our AC-AM channel at Ri $10^9\ \Omega$ (substrate voltages of 5–50 mV DC) were either nonexistent, or very similar to the DC and unfiltered AC channels, regardless of substrate voltage. It was clear that the output was R-plus-emf, not R-only. The lower the Ri level chosen, the more distorted the waveforms would be compared with the other channels. Presumably, this was because R components represented a higher proportion of the total signal, even with low substrate voltages (see emf/R responsiveness curve, below), and were over-emphasized by the filter. Also, waveform output was achieved only with enormous gains, at least 5000 times the gain levels used in the other channels. We concluded that the waveforms at higher Ri levels were the small, remnant emf waveforms that would be retained under the filter's "skirts" (described in Backus et al., 2000), since a true brickwall filter does not exist in modern electrical engineering. Because our monitor design incorporates very large gains and high resolution, it was possible to resolve remnants that were probably present but unresolvable by Tjallingii's AC–DC monitor. Only with much higher substrate voltages (such as the fixed 800 mV in the Tjallingii monitor) would the R component be large enough at Ri $10^9\ \Omega$ to be emphasized (relative to the emf remnant) after passage through the filter.

The Tjallingii AM-AC channel produced output waveforms at Ri $10^9\ \Omega$ that were different from those of its DC channel (Kindt et al., 2006). Due to this monitor's high, fixed substrate voltage and small gain capabilities, plus the tiny size of thrips, its AM-AC output probably did contain 100% of whatever small amount of R would be present at $10^9\ \Omega$ Ri. Due to the emf/R responsiveness curve, discussed below, the R component present at Ri $10^9\ \Omega$ is only a tiny fraction of the R at a lower Ri level. The small proportion resolvable at $10^9\ \Omega$ may not be biologically valuable, as Kindt et al. (2006) found. Additionally, to design a filtered AM-AC channel for our AC–DC Correlation Monitor that would achieve the goal of R-only signal output for any-sized arthropod, very high substrate voltages (potentially damaging to large insects) and low gain levels would have to be experimentally determined for each species at each Ri level. These settings also would have to be different for the filtered vs. unfiltered AC channels. We presently believe that such a design goal is unfeasible, while retaining the present value of flexible input impedances and substrate voltage type. Thus, use of flexible input impedances to record the full suite of R-only waveforms at lower Ri levels, according to the emf/R responsiveness curve is the best, most accurate way to provide users with more biologically valuable and complete R-only waveforms.

4.2. The emf/R responsiveness curve

Interpretation of the differences in waveforms among input resistor (Ri) levels described in Section 3 depends upon understanding the relationship among the three most important properties of the monitor-plant-insect circuit: (1) input impedance, Ri; (2) the insect's inherent resistance (Ra, in Tjallingii's terminology, Tjallingii, 1985); and (3) the emf/R responsiveness curve (Tjallingii, 1985, 1988). These properties also explain why it is necessary to design a monitor with flexibility in Ri level via switchable input impedances, in order to optimize waveform detail in recordings for any piercing–sucking insect.

Although Ra fluctuates with probing behavior, forming the waveform output (Walker, 2000), it fluctuates around a theoretical mean that varies for each species (Tjallingii, 1987). Generally, the larger the body size of a species, the lower its Ra. This is probably because stylet canal diameters are usually larger for larger insects

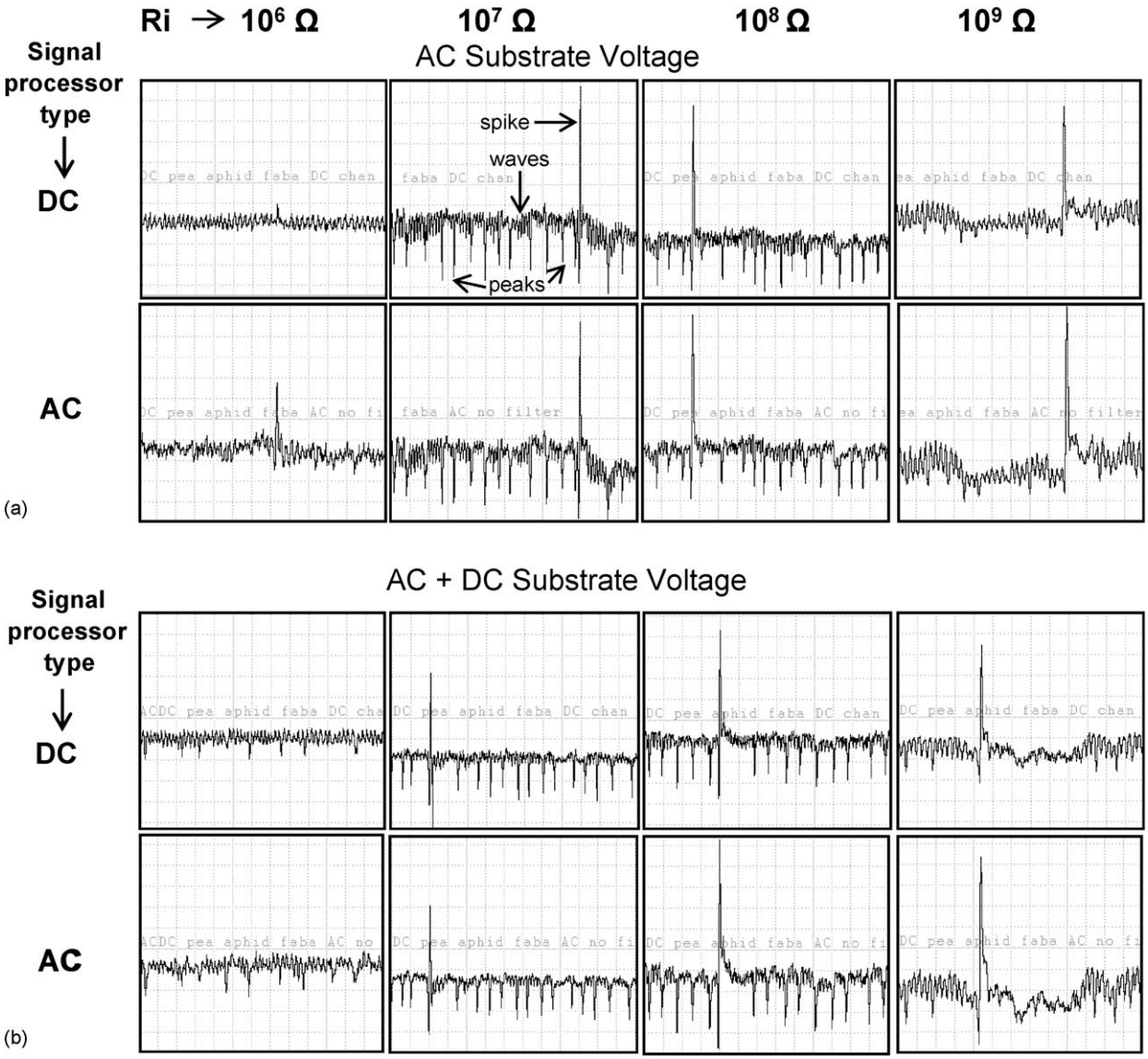

Fig. 7. (a) Pea aphid waveforms showing simultaneously outputted E2 waveform using AC substrate voltage. The two waveform excerpts in each column are simultaneous recordings of the same insect with different signal processing. Top row: DC signal processing channel, bottom row: AC channel. The AC channel had coupling capacitors switched off, and offset voltage used to remove rectifier fold-over of AC channel. Each column is from a different E2 excerpt, for each of four input resistor (Ri) levels from 10^6 to 10^9 Ω (columns). All waveforms are at Windaq compression level 5 (1.0 s/div), Windaq gain 16×. (b) Same for AC-plus-DC substrate voltage.

(although this is not always the case), and often the volume and/or conductivity of saliva changes with species (Walker, 2000). McLean calculated the Ra of the pea aphid (larger than most aphids) as 0.99 (i.e. nearly 1.0) × 10^8 Ω (McLean and Weigt, 1968). This explains why the most complete view of pea aphid waveforms occurred at 10^8 Ω Ri in our findings.

Tjallingii (1985, 1988) shows the importance of Ri when (using theoretical calculations based on Ohm's Law) he derives and explains the concepts of the R and emf components. These concepts are further explained and summarized in Walker (2000). In short, the greater the Ri of the amplifier, the more sensitive the amplifier is to emf components and less sensitive to R components. Thus, sensitivity to the two components is reciprocal. Tjallingii (1988) shows a chart of the voltage drop across the input resistor, Vi, in relation to the system voltage, *V* (i.e. Vi/*V*) plotted (on the *Y* axis) as a function of increasing log Ri levels (on the *X* axis). The result is a sigmoidal curve whose lag phase occurs at the lower Ri levels (Tjallingii, 1988). The log (rise) phase of the curve begins just below a species' Ra and its mid point is at Ra (e.g. about 10^8 Ω for the pea aphid) (Tjallingii, 1987). The curve plateaus out at higher Ri levels. This is Tjallingii's emf/R responsiveness curve (Tjallingii, 1988; termed the 'emf responsiveness curve' therein, but renamed herein for greater accuracy). As Vi/*V* approaches 1, emf responsiveness approaches 100% and R responsiveness approaches 0%; as Vi/*V* approaches zero, R responsiveness approaches 100% and emf approaches 0%. Thus, regardless of type of signal processing type used, emf will be emphasized at high Ri levels, while R will be emphasized at low Ri. This explains why the rapid drop and rise of the pd (sub-phases I and III) appear so abruptly and clearly at Ri 10^9 Ω (compared with Ri 10^8 Ω), because they are primarily emf component. Each insect has its own, unique Ra; therefore, each also has a unique emf/R responsiveness curve. Generally, responsiveness curves shift to the left (towards lower Ri) for larger insects and to the right (towards higher Ri) for smaller insects (Tjallingii, 1987).

To achieve the greatest balance of R:emf (ideally, 50:50), one should match as closely as possible the Ri level of the monitor to the Ra of the species of interest. Because most aphids are smaller

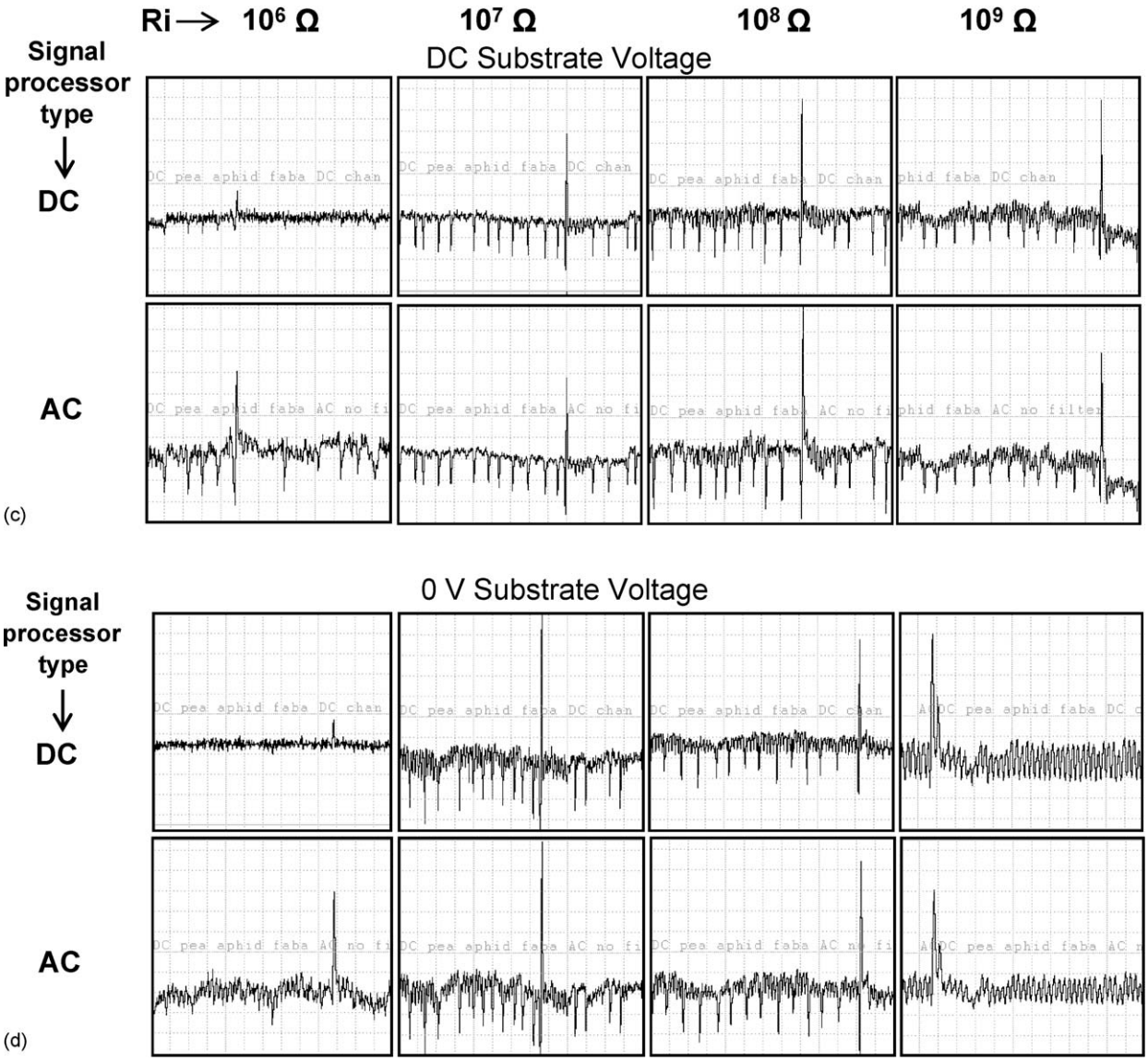

Fig. 7. Pea aphid E2 waveforms. (c) Same for DC substrate voltage. (d) Same for 0 V substrate voltage. Pale gray lettering is user annotation verifying channel identity.

than pea aphids and have an Ra just below $10^9\ \Omega$, that Ri level was chosen by Tjallingii as the standard level for the DC monitor (Tjallingii, 1988). Therefore, in order to optimize depth and breadth of waveform details for both R and emf, a universal monitor must have switchable input resistors, so that researchers can empirically measure and set Ri to Ra for their species of interest.

4.3. An AC monitor can be designed to detect emf

The results herein leave no doubt that AC signal processing can be designed to detect emf to the same level of detail as using DC signal processing. The most visually compelling evidence for this is that the AC channel displays waveforms whose electrical origin is primarily emf at Ri $10^9\ \Omega$ (i.e. pd and E2), regardless of whether an AC or DC signal processing is used. These emf waveforms are distinctly visible and nearly identical to classical DC waveforms in the literature. In fact, our results also show that the Missouri AC monitor could detect emf, although uncompensated rectifier fold-over and coupling capacitors caused distortion of signals below 0 V.

The strongest evidence that AC signal processing in the present monitor design can retain emf is that emf waveforms are also visible at Ri $10^{13}\ \Omega$, using both AC and DC signal processing and 0 V substrate (i.e. with only the electrode potential driving the signal). Ri levels of 10^{11}–$10^{15}\ \Omega$ have been used by Tjallingii and colleagues in special "emf only" head stage amplifiers, which are now considered the definitive test of emf (Lett et al., 2001). Waveforms whose electrical origin is 100% emf could only register in the AC signal processing channel if such waveforms were detectable by that circuitry. Therefore, it is particularly significant that waveform E2 is clearly recorded by the AC channel. E2 waves are considered in the DC literature to be one of the aphid waveforms whose electrical origin is most highly emf (Tjallingii and Prado, 2001). Until now, no EPG circuit design with AC signal processing has been capable of detecting E2 (personal observation, and Tjallingii, 1995).

4.4. How AC signal processing detects emf

It has been frequently reported that AC monitors cannot detect emf-component waveforms (e.g. Tjallingii, 2000), yet we have shown than an AC monitor can do this. There are two keys to explaining this. First, our AC signal processing, unlike that of previous monitor versions, was designed to retain emf. The AC–DC

Correlation Monitor compensates for rectifier fold-over, and completely removes all filters and coupling capacitors. This is important because AC carrier waves are affected by variations in voltage *in two ways*, modulation and summation (Backus et al., 2000). The R component will modulate the carrier wave, but any emf present at the measuring point of the primary circuit (i.e. the input resistor, Ri), will also summate the carrier (mentioned in Tjallingii, 1985, 2000). As more fully explained in Backus et al. (2000), AC amplifiers can detect summation effects because summation frequencies are very different from the 1000 Hz carrier wave's modulation. While only modulation frequencies are "carried" by the carrier, summation frequencies exist "outside" the carrier. Both effects will be combined in the primary circuit. If no filters exist downstream of the measuring point, then ultimately the emf is translated into the output waveform when the rectifier "draws" the envelope of the carrier (as explained in Backus and Bennett, 1992).

The second key is the emf/R responsiveness curve. Ri level dictates the proportion of R:emf that is present, with an optimal balance occurring when Ri = Ra. This is demonstrated by the responsiveness curve plotted for each species. Thus, the proportion of emf summation frequencies retained in the final output waveform will be determined by the responsiveness of a chosen Ri to emf, for the recorded insect species. This is why both types of signal processing can detect pure emf of pea aphid waveforms when Ri is $10^{13}\ \Omega$, but very little or none at all at $10^{6}\ \Omega$. Although deduced theoretically by Tjallingii nearly 30 years ago, our work is the first to demonstrate this empirically, for either AC or DC monitors.

It is interesting that our findings demonstrate a slight difference in detection of emf at $10^{9}\ \Omega$ Ri for DC vs. AC substrate voltage; both AC and DC signal processing were a bit more sensitive to emf using DC-only substrate voltage (e.g. compare the size of E2 peaks in Fig. 7b vs. c). Although this has not been tested electronically, perhaps DC substrate voltage is inherently more sensitive to summation-like effects than is an AC carrier wave. At the opposite end of the Ri spectrum, AC signal processing slightly accentuated R at Ri $10^{6}\ \Omega$, regardless of substrate voltage (e.g. compare the size of E2 spikes in Fig. 7a, DC vs. AC signal processing). These differences further justify the need for flexible Ri levels and substrate voltage types, so that users can choose settings that work best for their experimental needs. For example, Backus et al. (in press) chose $10^{8}\ \Omega$ Ri, DC signal processing, and AC substrate voltage for their correlation study of the C (ingestion) and B1 (salivation/precibarial valve fluttering) waveforms of *Homalodisca liturata* sharpshooters (Cicadellidae: Cicadellinae), because those settings emphasized emf while still retaining some R component for that species' waveforms.

4.5. Conclusions

The most important, overall conclusion from studies with the new AC–DC Correlation Monitor is that an AC monitor can be designed to detect emf- as well as R-component waveforms, and to reproduce them with high fidelity to the DC system's output waveforms. Therefore, the evidence described herein corrects a misconception prevalent among many EPG users (e.g. Zehnder et al., 2001; Prado and Tjallingii, 1997). This achievement will allow emf components to be recorded and rigorously studied for species that may be DC-sensitive, such as very large auchenorrhynchans, heteropterans, ticks, etc., especially those with inherent resistance levels less than $10^{8}\ \Omega$. Such a design leap was first predicted by the empirical circuit analysis described in Backus et al. (2000).

The key difference between most of the older AC designs and the DC system was probably the proportion of emf vs. R present at the measuring point, caused by different input resistor (Ri) values. In the earliest models, the presence of filters before the rectifier also eliminated emf (Backus et al., 2000). These filters were never present in the Missouri monitor. However, coupling capacitors (not exactly the same as filters) installed between the amplifier stages in the Missouri monitor, when combined with full-wave rectification, caused the emf waveforms to invert and/or elevate (although emf was still present, but distorted). These seemingly small differences, in fact, were the only monitor design characteristics that caused the AC and DC monitors' waveforms to differ. Yet the waveforms looked so distinctly different that they were thought to be impossible to reconcile. Our key finding to support this conclusion was that, when filters and coupling capacitors were removed and all other recording conditions were held constant *except* Ri, AC and DC pea aphid waveforms were virtually identical within each Ri level. In fact, both types of waveforms resembled high-resolution (computerized) Missouri AC monitor waveforms at $10^{6}\ \Omega$ Ri (albeit, without capacitor/rectifier effects) while both resembled high-resolution recordings of DC Tjallingii waveforms at $10^{9}\ \Omega$ Ri (Backus, unpublished data).

We conclude that when using the AC–DC Correlation Monitor, there is now no difference between AC and DC signal processing for pea aphid waveforms. Therefore, either circuitry can be used interchangeably, after taking into consideration possible insect sensitivity to type of substrate voltage. Tests with other aphid and non-aphid species are underway. To date, there appear to be virtually no differences within Ri level between waveforms from AC or DC signal processing for these other insects as well.

It would have been very difficult for earlier researchers to determine these key conclusions. Seven different monitor designs and many different recording conditions have been used over the last 45+ years of insect monitoring. Equally importantly, Tjallingii (1985, 2000) was correct in pointing out that issues outside the monitor design such as slow-response strip chart recorders and absence of Faraday cages were problematic. When we held these minor but nagging differences constant (by eliminating filters, using high-quality, well-grounded Faraday cages, and precision, high-resolution A/D equipment), we found that the remaining differences in waveform appearance between monitor designs were not only primarily explained by Ri level, but also by filters, coupling capacitors, and rectifier fold-over.

4.6. Advantages of using the AC–DC Correlation Monitor

Introduction of the AC–DC Correlation Monitor design is not intended to render obsolete the use of the Tjallingii DC monitor. On the contrary, our intent is to emulate the success of that monitor for more diverse species. We add more flexibility of monitor settings in order to apply Tjallingii's own findings on the emf/R responsiveness curve. Thus, for larger arthropods with inherent resistances lower than $10^{9}\ \Omega$, restricting amplifier sensitivity to $10^{9}\ \Omega$ Ri will over-emphasize emf-component waveforms (e.g. Lett et al., 2001, found exclusively emf-component waveforms), compared with a theoretical optimum that would be achieved with a more flexible system. Numerous studies have shown the value of R-component waveforms, and the need for balanced R/emf detection. Thus, while recent studies using the Tjallingii DC monitor for auchenorrhynchans demonstrate that this monitor can be used for such insects, their output waveforms are not optimal.

EPG researchers who presently own a DC Tjallingii monitor may continue to use it, especially for studies of small insects such as sternorrynchans, whose inherent Ra is near $10^{9}\ \Omega$. However, those scientists working with larger arthropods, or who wish to study multiple, diverse arthropod species including (but not limited to) sternorrynchans, should strongly consider using the new AC–DC Correlation Monitor. After all, a researcher can perfectly duplicate

the settings of the Tjallingii DC monitor and its output waveforms using the AC–DC Correlation Monitor, plus try out other settings. In addition to its more flexible settings and choice of substrate voltage types, the present design is a greatly improved electronic device compared to the 30-year-old Tjallingii DC monitor, with updated, precision components designed for high-quality signal output. These improvements are designed to solve the DC Tjallingii monitor's problems, such as: voltage artifacts; insufficient gain for larger insects; poor regulation, compensation and reproducibility of substrate voltages; and others.

With our AC–DC Correlation Monitor, four new types of studies are made possible. First, a researcher whose study insect was first recorded many years ago with an AC monitor can update the published waveforms by dynamically comparing a fresh model of older signals with today's modern signals, using whichever type of substrate voltage (and signal processing) that best suits the sensitivity of the study insect. Second, if an insect has never been EPG-recorded before, a researcher can quickly and easily compare all possible settings and recording methods, to determine which works best for that species.

Both types of studies are already underway in labs now using the AC–DC Four-channel monitor (described below). A diverse array of insect species has been successfully recorded with the new monitor design, with manuscripts currently *in press* or *in preparation*. These insects include chinch bug, *Blissus insularis* Barber (Heteroptera: Blissidae) (Rangasamy, 2007), squash bug, *Anasa tristis* (De Geer) (Heteroptera: Coreidae) (A. Wayadande, unpublished data), southern green stinkbug, *Nezara viridula* (Linnaeus) (Heteroptera: Pentatomidae) (P. Mitchell, unpublished data), corn leafhopper, *Dalbulus maidis* (DeLong and Walcott) (Carpane, 2007), blackfaced leafhopper, *Graminella nigrifrons* (Forbes) (M. Redinbaugh, unpublished data), beet leafhopper, *Circulifer tenellus* (Baker) (A. Wayadande, unpublished data), several species of *Homalodisca* spp. sharpshooters (e.g. Dugravot et al., 2008; Backus et al., in press) (all Auchenorrhyncha: Cicadellidae), as well as soybean aphid, *Aphis glycines* Matsumura (M. Redinbaugh, unpublished data) and cotton-melon aphid, *Aphis gossypii* Glover (Backus, unpublished data) (both Sternorrhyncha: Aphididae). Future studies are planned for ticks, biting flies (A. Li, personal communication) and ovipositing hymenopterans (B. Vinson, personal communication).

A third type of study made possible by the AC–DC Correlation Monitor is to compare waveform outputs at different Ri levels, for a new way to determine the relative contribution of R and emf to each waveform type, and thereby hypothesize a waveform's biological meaning. This is possible today because biological correlations are now established for many R-component waveforms (e.g. various types of salivation, or valves opening and closing; Walker, 2000) vs. emf-component waveforms (e.g. membrane potentials upon penetrating the plasmalemma [Walker, 2000], or streaming potentials of fluid moving through stylets [Dugravot et al., 2008]). Such comparisons can speed up waveform correlation work for new species. Finally, a fourth type of study would be to explore new questions for species that have previously been recorded using other monitors. For example, aphid researchers may wish to better correlate pathway waveforms with specific stages of salivary sheath formation (a dominant R waveform), as has been done for sharpshooter leafhoppers (Backus et al., 2005). This can be now done by lowering the Ri to 10^6 or $10^7\ \Omega$, to increase the R responsiveness for aphids. Additionally, sensitivity to AC vs. DC substrate voltages, and many other questions, can be easily addressed and answered.

In addition to the AC–DC Correlation Monitor, Bennett and Backus have also developed an AC–DC Four-channel monitor, for multiple-insect recordings. The circuitry for that monitor is very similar to the AC–DC Correlation Monitor, but provides individual recording channels for up to four insects. Thus, multiple-insect comparisons can be made using an insect's empirically determined, optimum substrate voltage type and Ri level.

Acknowledgments

We thank Holly Shugart and Jose Gutierrez for rearing plants and insects for this study. We also are grateful to Dr. Jack Dillwith (Oklahoma State University) for kindly providing faba bean-conditioned pea aphids for our colony (imported into California under USDA-APHIS permit no. P526P-06-01824). Greg Walker (UC Riverside) and Astri Wayadande (Oklahoma State University) made substantive and helpful suggestions to earlier drafts of the manuscript, which we gratefully acknowledge. We also appreciate the comments of three anonymous reviewers. This work was funded by USDA ARS in-house funds and a grant from the University of California Pierce's Disease Research Program.

References

Backus, E.A., 1994. History, development, and applications of the AC electronic monitoring system for insect feeding. In: Ellsbury, M.M., Backus, E.A., Ullman, D.L. (Eds.), History, Development, and Application of AC Electronic Insect Feeding Monitors. Entomological Society of America, Lanham, MD, pp. 1–51.

Backus, E.A., Bennett, W.H., 1992. New AC electronic insect feeding monitor for fine-structure analysis of waveforms. Annals of the Entomological Society of America 85, 437–444.

Backus, E.A., Cline, A.R., Ellersieck, M.R., Serrano, M.S., 2007. *Lygus hesperus* (Knight) (Hemiptera: Miridae) feeding on cotton: New methods and parameters for analysis of non-sequential EPG data. Annals of the Entomological Society of America 100, 296–310.

Backus, E.A., Devaney, M.J., Bennett, W.H., 2000. Comparison of signal processing circuits among seven AC electronic monitoring systems for their effects on the emf and R components of aphid (Homoptera: Aphididae) waveforms. In: Walker, G.P., Backus, E.A. (Eds.), Principles and Applications of Electronic Monitoring and other Techniques in the Study of Homopteran Feeding Behavior. Entomological Society of America, Lanham, MD, pp. 102–143.

Backus, E.A., Habibi, J., Yan, F., Ellersieck, M.R., 2005. Stylet penetration by adult *Homalodisca coagulata* on grape: Electrical Penetration Graph waveform characterization, tissue correlation, and possible implications for transmission of *Xylella fastidiosa*. Annals of the Entomological Society of America 98, 787–813.

Backus, E.A., Holmes, W., Schreiber, F., Reardon, B.F., Walker, G.P. Sharpshooter X wave: correlation of an EPG waveform with xylem ingestion supports a hypothesized mechanism for *Xylella fastidiosa* inoculation. Annals of the Entomological Society of America, in press.

Bonjour, E.L., Fargo, W.S., Webster, J.A., Richardson, P.E., Brusewitz, G.H., 1991. Probing behavior comparisons of squash bugs (Heteroptera: Coreidae) on cucurbit hosts. Environmental Entomology 20, 143–149.

Buduca, C., Reynaud, B., Lan Sun Luk, D., Molinaro, F., 1996. Electrical penetration graphs from *Peregrinus maidis* on a susceptible maize hybrid. Entomologia Experimentalis et Applicata 79, 131–139.

Calatayud, P.A., Seligmann, C.D., Polania, M.A., Bellotti, A.C., 2001. Influence of parasitism by encyrtid parasitoids on the feeding behavior of the cassava mealybug *Phenacoccus herreni*. Entomologia Experimentalis et Applicata 98, 271–278.

Carpane, P.D., 2007. Host resistance and diversity of *Spiroplasma kunkelii* as components of corn stunt disease. Ph.D. Dissertation. Oklahoma State University. 110 pp.

Dugravot, S., Backus, E.A., Reardon, B.F., Miller, T.A., 2008. Correlations of cibarial muscle activities of *Homalodisca* spp. sharpshooters (Hemiptera: Cicadellidae) with EPG waveforms and excretion. Journal of Insect Physiology 54, 1467–1478.

Fereres, A., Collar, J.L., 2001. Analysis of noncirculative transmission by electrical penetration graphs. In: Harris, K.F., Smith, O.P., Duffus, J.E. (Eds.), Virus-Insect-Plant Interactions. Academic Press, New York, NY, pp. 87–109.

Harrewijn, P., Tjallingii, W.F., Mollema, C., 1996. Electrical recording of plant penetration by western flower thrips. Entomologia Experimentalis et Applicata 79, 345–353.

Janssen, J.A.M., Tjallingii, W.F., van Lenteren, J.C., 1989. Electrical recording and ultrastructure of stylet penetration by the greenhouse whitefly. Entomologia Experimentalis et Applicata 52, 69–81.

Kawabe, S., McLean, D.L., Tatsuki, S., Ouchi, T., 1981. An improved electronic measurement system for studying ingestion and salivation activities of leafhoppers. Annals of the Entomological Society of America 74, 222–225.

Kimmins, F.M., Bosque-Perez, N.A., 1996. Electrical penetration graphs from *Cicadulina* spp. and the inoculation of a persistent virus into maize. Entomologia Experimentalis et Applicata 80, 46–49.

Kindt, F., Joosten, N.N., Peters, D., Tjallingii, W.F., 2003. Characterisation of the feeding behaviour of western flower thrips in terms of electrical penetration graph (EPG) waveforms. Journal of Insect Physiology 49, 183–191.

Kindt, F., Joosten, N.N., Tjalingii, W.F., 2006. Electrical penetration graphs of thrips revised: combining DC- and AC-EPG signals. Journal of Insect Physiology 52, 1–10.

Kingston, K.B., 2007. Digestive and feeding physiology of grape phylloxera (*Daktulosphaira vitifoliae* Fitch). Ph.D. Dissertation. The Australian National University, Canberra, ACT, Australia, p. 400.

Lett, J.M., Granier, M., Grondin, M., Turpin, P., Molinaro, F., Chiroleu, F., Peterschmitt, M., Reynaud, B., 2001. Electrical penetration graphs from *Cicadulina mbila* on maize, the fine structure of its stylet pathways and consequences for virus transmission efficiency. Entomologia Experimentalis Et Applicata 101, 93–109.

McLean, D.L., Kinsey, M.G., 1964. A technique for electronically recording aphid feeding and salivation. Nature 202, 1358–1359.

McLean, D.L., Weigt, W.A., 1968. An electronic measuring system to record aphid salivation and ingestion. Annals of the Entomological Society of America 61, 180–185.

Miranda, M.P., Fereres, A., Appezzato-Da-Gloria, B., Lopes, J.R.S., 2009. Characterization of electrical penetration graphs of *Bucephalogonia xanthophis*, a vector of *Xylella fastidiosa* in citrus. Entomologia Experimentalis et Applicata 130, 35–46.

Prado, E., Tjallingii, W.F., 1997. Effects of previous plant infestation on sieve element acceptance by two aphids. Entomolgia Experimentalis et Applicata 82, 189–200.

Rangasamy, M., 2007. Mechanisms of resistance to southern chinch bug, *Blissus insularis* Barber (Hemiptera: Blissidae), in St. Augustinegrass. Ph.D. Dissertation. University of Florida, 126 pp.

Reese, J., Tjallingii, W.F., Van Helden, M., Prado, E., 2000. Waveform comparisons among AC and DC electronic monitoring systems for aphid (Homoptera: Aphididae) feeding behavior. In: Walker, G.P., Backus, E.A. (Eds.), Principles and Applications of Electronic Monitoring and other Techniques in the Study of Homopteran Feeding Behavior. Entomological Society of America, pp. 70–101.

Serrano, M.S., Backus, E.A., Cardona, C., 2000. Comparison of AC electronic monitoring and field data for estimating tolerance to *Empoasca kraemeri* (Homoptera: Cicadellidae) in common bean genotypes. Journal of Economic Entomology 93, 1796–1809.

Stafford, C.A., Walker, G.P., 2009. Characterization and correlation of DC electrical penetration graph waveforms with feeding behavior of beet leafhopper, *Circulifer tenellus*. Entomologia Experimentalis et Applicata 130, 113–129.

Stafford, C.A., Walker, G.P., Creamer, R., 2009. Stylet penetration behavior resulting in inoculation of beet severe curly top virus by beet leafhopper, *Circulifer tenellus*. Entomologia Experimentalis et Applicata 130, 130–137.

Tjallingii, W.F., 1978. Electronic recording of penetration behaviour by aphids. Entomologia Experimentalis et Applicata 24, 721–730.

Tjallingii, W.F., 1985. Electrical nature of recorded signals during stylet penetration by aphids. Entomologia Experimentalis et Applicata 38, 177–186.

Tjallingii, W.F., 1987. Backus's Lecture Notes on the Nature of Electrical Signals in EPG. 1st International EPG Summer School, Wageningen, Netherlands.

Tjallingii, W.F., 1988. Electrical recording of stylet penetration activities. In: Minks, A.K., Harrewijn, P. (Eds.), Aphids: Their Biology, Natural Enemies and Control. Elsevier, Amsterdam, pp. 95–108.

Tjallingii, W.F., 1995. Regulation of phloem sap feeding by aphids. In: Chapman, R.F., de Boer, G. (Eds.), Regulatory Mechanisms in Insect Feeding. Chapman & Hall, New York, NY, pp. 190–209.

Tjallingii, W.F., 2000. Comparison of AC and DC systems for electronic monitoring of stylet penetration activities by homopterans. In: Walker, G.P., Backus, E.A. (Eds.), Principles and Applications of Electronic Monitoring and other Techniques in the Study of Homopteran Feeding Behavior. Entomological Society of America, pp. 41–69.

Tjallingii, W.F., Gabrys, B., 1999. Anomalous stylet punctures of phloem sieve elements by aphids. Entomologia Experimentalis et Applicata 91, 97–103.

Tjallingii, W.F., Prado, E., 2001. Analysis of circulative transmission by electrical penetration graphs. In: Harris, K.F., Smith, O.P., Duffus, J.E. (Eds.), Virus-Insect-Plant Interactions. Academic Press, San Diego, CA.

Velusamy, R., Heinrichs, E.A., 1986. Electronic monitoring of feeding behavior of *Nilaparvata lugens* (Homoptera: Delphacidae) on resistant and susceptible rice cultivars. Environmental Entomology 15, 678–682.

Walker, G.P., 2000. Beginner's guide to electronic montioring. In: Walker, G.P., Backus, E.A. (Eds.), Principles and Applications of Electronic Monitoring and other Techniques in the Study of Homopteran Feeding Behavior. Entomological Society of America, pp. 14–40.

Walker, G.P., Backus, E.A., 2000. Principles and Applications of Electronic Monitoring and other Techniques in the Study of Homopteran Feeding Behavior. Entomological Society of America, Lanham, MD, 260 pp.

Walker, G.P., Janssen, J.A.M., 2000. Electronic recording of whitefly (Homoptera: Aleyrodidae) feeding and oviposition behavior. In: Walker, G.P., Backus, E.A. (Eds.), Principles and Applications of Electronic Monitoring and other Techniques in the Study of Homopteran Feeding Behavior. Entomological Society of America, pp. 172–200.

Wayadande, A.C., Nault, L.R., 1993. Leafhopper probing behavior associated with maize chlorotic dwarf virus transmission to maize. Phytopathology 83, 522–526.

Zehnder, G.W., Nichols, A.J., Edwards, O.R., Ridsdill-Smith, T.J., 2001. Electronically monitored cowpea aphid feeding behavior on resistant and susceptible lupins. Entomologia Experimentalis et Applicata 98, 259–269.